Title

CRISPR-based screens uncover determinants of immunotherapy response and potential combination therapy strategies

Authors and affiliations

Poornima Ramkumar[1], Ruilin Tian[1], Meghan Seyler[1], Jaime T. Leong[1], Merissa Chen[1], Priya Choudhry[2], Torsten Hechler[3], Nina Shah[4], Sandy W. Wong[4], Tom G. Martin III[4], Jeffrey L. Wolf[4], Kole T. Roybal[5,6,7,8], Andreas Pahl[3], Jack Taunton[9], Arun P. Wiita[2,8], Martin Kampmann[1,7,8,10]

[1]Institute for Neurodegenerative Diseases, University of California, San Francisco, CA, USA
[2]Department of Laboratory Medicine, University of California, San Francisco, CA, USA
[3] Heidelberg Pharma, Schriesheimer Str. 101, 68526 Ladenburg, Germany
[4] Division of Hematology/Oncology, Department of Medicine, University of California, San Francisco, CA, USA
[5] Department of Microbiology and Immunology, University of California, San Francisco, San Francisco, CA, USA
[6]Parker Institute for Cancer Immunotherapy, San Francisco, CA, USA
[7]Chan-Zuckerberg Biohub, San Francisco, CA, USA
[8]Helen Diller Family Comprehensive Cancer Center, University of California, San Francisco, CA, USA
[9]Department of Cellular and Molecular Pharmacology, University of California, San Francisco, San Francisco, CA, USA
[10]Department of Biochemistry and Biophysics, University of California, San Francisco, San Francisco, CA, USA

Corresponding Author:

Martin Kampmann, University of California, San Francisco, 675 Nelson Rising Lane, San Francisco CA 94158, USA. Email: martin.kampmann@ucsf.edu, Phone: 415-514-5545.

Financial Support

This work was supported by a Postdoctoral Fellowship from the UCSF Program for Breakthrough Biomedical Research (to P.R.), K99/R00 CA181494 (to M.K.), a Stand Up to Cancer Innovative Research Grant (to M.K.), the UCSF Stephen and Nancy Multiple Myeloma Translational Initiative (to M.K., K.T.R, A.P.W), UCSF Breast Cancer Research Funds (to J.T.), R01 CA226851 (to A.P.W.).

Disclosure of potential conflict of interest

M.K. has filed a patent application related to CRISPRi and CRISPRa screening (PCT/US15/40449) and serves on the Scientific Advisory Board of Engine Biosciences.
A.P. and T.H. are employed at Heidelberg Pharma (A.P.) and Heidelberg Pharma Research GmbH (T.H.) and are working on the development of Amatoxin based ADCs (including HDP-101). Heidelberg Pharma holds patents concerning the conjugation of Amatoxins to antibodies.
K.T.R is a cofounder and stockholder in Arsenal Biosciences. K.T.R was a founding scientist/consultant and stockholder in Cell Design Labs now a Gilead Company. K.T.R holds stock in Gilead. J.T. is a cofounder and shareholder of Global Blood Therapeutics, Principia

Biopharma, Kezar Life Sciences, and Cedilla Therapeutics. J.T. is listed as an inventor on a provisional patent application describing PS3061. A.P.W. is a member of the scientific advisory board and equity holder in Protocol Intelligence, LLC, and Indapta Therapeutics, LLC.

Word Count: 6,210
Total number of figures and tables: 7

Abstract:

Cancer cells commonly develop resistance to immunotherapy, commonly by loss of antigen expression. Combinatorial treatments that increase levels of the target antigen on the surface of cancer cells have the potential to restore efficacy to immunotherapy. Here, we use our CRISPR interference and CRISPR activation-based functional genomics platform to systematically identify pathways controlling cell-surface expression of the multiple myeloma immunotherapy antigen BCMA. We discovered that inhibition of HDAC7 and the Sec61 complex increased cell-surface BCMA, including in primary patient cells. Importantly, pharmacological Sec61 inhibition enhanced the anti-myeloma efficacy of a BCMA-targeted antibody-drug conjugate. A CRISPR interference CAR-T coculture screen enabled us to identify both antigen-dependent and -independent mechanisms controlling response of myeloma cells to BCMA-targeted CAR-T cells. Thus, our study demonstrates the potential of CRISPR screens to uncover mechanisms controlling response of cancer cells to immunotherapy and to suggest potential combination therapies.

Statement of significance:
Cancer patients can acquire resistance to immunotherapy, often by reducing expression of the targeted antigen. Using CRISPR screens, we systematically identified mechanisms increasing expression of the immunotherapy target BCMA and efficacy of a BCMA-directed antibody drug conjugate. We also identified antigen-independent mechanisms regulating response of cancer cells to CAR-T cells.

Introduction:
Immunotherapy has transformed the treatment of many types of cancer. As with other therapeutic strategies, emergence of treatment-resistant cancer cells remains a major challenge. CRISPR-based genetic screens are a powerful research tool to define mechanisms of treatment resistance in cancer cells, and to design strategies to overcome resistance. CRISPR screens have recently been applied to define cellular mechanisms by which cancer cells can regulate the levels of programmed cell death ligand 1 (PD-L1) (1), which in turn determines the response to anti-PD-L1 therapy, and to identify factors controlling the sensitivity to CD22-targeted antibody-drug-conjugates (ADCs) (2).

An important mechanism by which cancer cells can become resistant to different forms of immunotherapy in the clinic, including monoclonal antibodies, ADCs, and chimeric antigen receptor T (CAR-T) cells, is the downregulation or loss of the targeted antigen (3) (4), also termed “antigen escape”. Preclinical studies have demonstrated that resistance due to antigen loss can be rescued by combining drugs that function to upregulate antigen gene expression (3,5,6). Additionally, pharmacological strategies to increase antigen expression have shown promise in improving responses to immunotherapy (5,6). Therefore, we reasoned that genome-wide CRISPR-based screens designed to identify mechanisms for upregulation of specific antigens would be a systematic and scalable approach to identify such combinatorial treatments.

Here we apply this strategy to an immunotherapy target in multiple myeloma, B cell maturation antigen (BCMA) encoded by the *TNFRSF17* gene. BCMA is expressed on the cell surface of myeloma cells, plasma cells and some mature B cells (7)) and not detected in other normal tissue, making it an attractive immunotherapy target for multiple myeloma (8). BCMA

protein belongs to the tumor necrosis factor receptor (TNFR) superfamily, along with B-cell activation factor receptor (BAFF-R) and transmembrane activator and calcium modulator and cyclophilin ligand interactor (TACI) (8). By binding to their ligands a proliferation-inducing ligand (APRIL) and BAFF, they regulate B cell proliferation, survival and differentiation into plasma cells (8). Recent studies have shown that membrane-bound BCMA (mBCMA) is cleaved on the cell surface by the gamma-secretase complex to a soluble form of BCMA (sBCMA) that includes the extracellular domain and a small part of the transmembrane domain (9).

BCMA is currently being evaluated in numerous clinical trials as an immunotherapy target in multiple myeloma (8). BCMA-targeted immunotherapy agents have shown improved responses in relapsed and refractory patients (10,11). However, as with other multiple myeloma therapies, resistance and relapse to BCMA-targeted therapies has emerged as a significant challenge and presents an unmet need (12,13). Ongoing clinical trials using BCMA-targeted chimeric antigen receptor T cells (CAR-T cells) have reported antigen loss in some patients undergoing relapse (12,13), indicating that reduced cell-surface levels of BCMA may be an important mechanism of therapy resistance. However, the underlying cellular mechanisms remain to be understood.

Therefore, our goal was to systematically elucidate the mechanisms by which the cell-surface expression of BCMA is controlled in myeloma cells, and to test whether some of these mechanisms would be potential targets for combination therapy to enhance BCMA-directed immunotherapy. Here, we use our CRISPR-interference/CRISPR-activation (CRISPRi/CRISPRa) functional genomics platform (14,15) to identify genes or pathways regulating cell surface levels of BCMA in multiple myeloma cells. Using this approach, we identified cellular mechanisms at the levels of transcription, post-translational trafficking and processing that selectively controlled cell-surface levels of BCMA, but not of another immunotherapy target in multiple myeloma, CD38. Pharmacological targeting of several hits from our genetic screen, including *HDAC7* and the Sec61 complex, upregulated cell surface BCMA in myeloma cell lines and patient samples. Moreover, inhibition of Sec61 complex increased the efficacy of BCMA-targeted antibody drug conjugate (ADC).

Furthermore, we conducted a CRISPRi screen for genes controlling sensitivity of multiple myeloma cells to BCMA-directed CAR-T cells. To our knowledge, this is the first genetic screen for genes in cancer cells controlling response to CAR-T cells directed against a clinically relevant target. This screen uncovered both antigen-dependent and antigen-independent mechanisms modulating sensitivity to BCMA-targeted CAR-T cells.

Our results demonstrate the potential of CRISPR screens to elucidate mechanisms controlling the response of cancer cells to immunotherapy and the identification of potential pharmacological strategies to enhance immunotherapy.

Results:

Genome-wide CRISPR screens to identify genes controlling cell surface BCMA expression

To identify novel genes or pathways regulating cell surface expression of BCMA in MM cell line, we performed genome-wide CRISPRi and CRISPRa screens in a multiple myeloma cell line (Fig 1A). To select a suitable cell line for these primary screens, we compared levels of BCMA expression on the RNA (www.keatslab.org) and cell surface protein levels for a panel of multiple myeloma cell lines (Fig. 1B). We found that AMO1 cells expressed moderate levels of cell

surface BCMA. We therefore selected this line for our primary screen as we reasoned it would enable us to identify modifiers that either increase or decrease BCMA surface levels (Fig 1B).

AMO1 cells were lentivirally transduced to express the CRISPRi and CRISPRa machinery and CRISPR functionality was tested using sgRNA targeted towards *CD38* and *CXCR4* respectively (Supplementary Fig S1). The genome-wide screen was conducted as shown in Fig 1A. Briefly, AMO1 cells expressing the CRISPRi and CRISPRa machinery were transduced with pooled genome-wide sgRNA library. The cells were then stained for cell surface BCMA using fluorescent tagged antibody and subjected to flow sorting into BCMA-low and BCMA-high populations. Frequencies of cells expressing each sgRNA were identified by next-generation sequencing. Using a stringent cut-off (false-discovery rate (FDR) ≤ 0.01), the genome-wide CRISPRi screen identified several genes regulating cell surface expression of BCMA (Fig. 1C and Supplementary Table S1). Knocking down BCMA itself or its transcription factor *POU2AF1* (16) both resulted in significant downregulation of cell surface BCMA expression, thus validating the screen (Fig 1C). Furthermore, all of the subunits of the gamma secretase complex were among the top hits, and their knockdown resulted in a significant increase in cell surface BCMA (Fig 1C), consistent with previous reports from other groups (6,9). Moreover, we identified several functional categories of genes regulating expression levels of BCMA including subunits of the Sec61 translocon complex, peroxisome biogenesis, proteasome subunits, and regulators of transcription (Fig 1C).

Our CRISPRa genome-wide screen (Fig. 1D and Supplementary Table S2) identified genes in the Mucin family (*MUC1*, *MUC21*) and several genes involved in transcriptional regulation (*POU2AF1*, *CBFA2T3*, *MAML2*, *RUNX3*) that regulated surface BCMA. Systematic comparison of the parallel CRISPRi and CRISPRa screens (Fig. 1E) revealed that overexpression and knockdown of some genes had opposing effects on BCMA surface levels – including BCMA itself and *POU2AF1*. However, other genes were hits in only the CRISPRi or CRISPRa screens, notably the subunits of the gamma secretase complex and the Sec61 complex; highlighting the fact that CRISPRi and CRISPRa screens can uncover complementary results, as we previously described in other systems (14).

Validation of hit genes in a panel of multiple myeloma cell lines

To test the generality of our findings, we decided to validate hit genes from the primary screen performed on the AMO1 cells in a panel of multiple myeloma lines, which we engineered to express CRISPRi machinery and in which we confirmed CRISPRi activity (Supplementary Fig. S1). We chose the top 50 hits with a significant phenotype from the CRISPRi screen for testing in this panel. The secondary screen was performed similarly to the genome-wide screen to validate changes in BCMA. The screen was carried out in parallel for a different cell surface protein expressed in all multiple myeloma lines, CD38, to investigate whether hit genes selectively affected BCMA expression, or more generally affected expression of several cell-surface proteins.

As observed in the primary CRISPRi screen, knockdown of the subunits of gamma secretase subunits significantly increased cell surface BCMA (Fig. 2A). We found this effect to be selective for BCMA, since gamma secretase knockdown had no effect on CD38 expression in a panel of MM cell lines (Fig 2A). This was further validated using a pharmacological inhibitor of gamma secretase complex, RO4929097 (17). MM cell lines treated with the indicated concentration of RO4929097 showed an increase in both BCMA cell surface expression by flow cytometry (Fig 2B) and in total protein levels of BCMA by immunoblotting (Fig 2C). Thus, we

were able to successfully validate genes from our primary screen in a panel of MM cell lines, using both genetic and pharmacological perturbations.

Several of the novel factors from our primary screen also validated in the larger panel of multiple myeloma cells (Fig. 2A and Supplementary Table S3), most notably the transcriptional regulator *HDAC7* and *SEC61A1*, a subunit of the SEC61 translocon. Knockdown of both factors increased cell-surface levels of BCMA, but not CD38 (Fig 2A).

Class II HDAC inhibition upregulates BCMA transcription

Our screen found that knockdown of *HDAC7* specifically increases cell-surface levels of BCMA in several multiple myeloma lines (Fig. 2A). *HDAC7* is a member of the histone deacetylase (HDAC) family, which have emerged as crucial transcriptional co-repressors(18). *HDAC7* belongs to the Class II family of HDACs, which are subdivided into Class IIa including *HDAC4,5,7,9* and Class IIb including *HDAC6* and *HDAC10* (18). We validated our screen findings using a pharmacological inhibitor targeting Class IIa HDACs, TMP269 (19). Treatment of RPMI8226 cells with increasing concentrations of TMP269 showed a two-fold increase in BCMA protein levels (Fig 3A-C). Because HDACs have been established to regulate transcription of several genes, we performed qPCR to analyze for changes in transcript levels of BCMA. Our results showed a two-fold increase in BCMA transcript levels (Fig 3D), indicating that Class II HDAC inhibition regulates transcription of BCMA. No significant change was observed in the CD38 protein or transcript levels (Fig 3A, 3D).

To investigate whether this change in BCMA levels is specific to Class IIa HDAC inhibition, we treated cells with a pan-HDAC inhibitor, panobinostat (20), and a HDAC6-specific inhibitor, ricolinostat (21) (Fig3A, 3D). Our results showed no increase in BCMA transcript levels with these agents. Furthermore, treatment with TMP269 in K562 cells, which do not express BCMA, did not lead to an increase in BCMA expression (Supplementary Fig S2). This finding suggests that TMP269 can enhance BCMA expression in cell types that naturally express it, but that it does not induce ectopic expression in other cell types at measurable levels. These results indicate the potential for using Class IIa HDAC inhibition to increase expression of BCMA in plasma cells in the context of BCMA-targeted immunotherapy without unintended effect on cell types that do not express BCMA.

The Sec61 translocon regulates BCMA protein levels

Most integral plasma membrane proteins are inserted into membranes via the Sec61 translocon, located in the endoplasmic reticulum. It has been shown that inhibition of Sec61 affects correct localization of a subset of membrane proteins, and that sensitivity is determined by the N-terminal signal peptide or first transmembrane domain(22,23). Surprisingly, our CRISPRi screen identified that knockdown of genes in the SEC61 pathway, such as the *SEC61A1*, *SEC61G*, *SSR1* and *OSTC*, resulted in an increase – rather than a decrease - in BCMA cell surface levels (Fig. 1C). This unexpected finding was confirmed in our validation screens in the panel of multiple myeloma cell lines (Fig. 2A). Conversely, *SEC61A1* knockdown resulted in a decrease in CD38 cell surface levels (Fig. 2A), as would be expected for most membrane proteins.

To test whether pharmacological inhibition of the Sec61 translocon complex phenocopies the genetic knockdown, we treated cells with SEC61 inhibitors, CT8 (22) and PS3061(24). We observed that treatment of MM cell lines with increasing concentrations of these compounds results in an up to five-fold dose-dependent increase in cell-surface BCMA levels and a decrease

in cell surface CD38 levels, as evidenced by flow cytometry (Figs. 4A, 4D, Supplementary Fig S3A). Moreover, immunoblotting also showed a dose-dependent increase in total BCMA protein levels (Fig. 4B, 4E, Supplementary Fig S3B) and up to two-fold increase in BCMA transcript levels (Fig. 4C, 4F). This change in transcript levels could be due to stabilization of mRNAs bound to ER-targeted ribosomes upon inhibition of the SEC61 complex. Furthermore, treatment of cells with SEC61 inhibitors resulted in a decrease in TACI, which, like BCMA, belongs to the TNFRSF family of proteins (Supplementary Fig S3C), indicating that the SEC61 inhibition selectively upregulates BCMA levels.

To uncover the mechanism by which SEC61 inhibition increases BCMA levels, we first tested the possibility that a reduction in gamma-secretase levels at the plasma membrane would reduce shedding of BCMA from the cell surface. Pharmacological inhibition of either the gamma-secretase or Sec61 resulted in increased cell surface BCMA as evidenced by flow cytometry (Fig. 4G). To determine levels of sBCMA generated by gamma-secretase processing, we performed sandwich ELISA assay on cells treated with PS3061 or gamma secretase inhibitor, RO4929097 for 24 hrs. Our results show that inhibition of gamma-secretase activity substantially reduced sBCMA levels, whereas we did not observe substantial changes in sBCMA levels with SEC61 inhibition (Fig 4H). This finding indicated that the increase in cell-surface BCMA is not driven by reduced shedding of BCMA. Further investigation is required to determine the mechanism by which SEC61 modulates BCMA cell surface expression.

To validate our findings in primary patient cells, we treated bone marrow mono-nuclear cells (BM-MNCs) derived from different MM patients (Supplementary Table S4) with increasing concentrations of TMP269 and RO4929097 for 24 hrs and analyzed the expression of BCMA on plasma cells by flow cytometry. We observed an up to 2.5-fold increase in cell-surface BCMA with class II HDAC inhibition and an up to 8-fold increase with gamma-secretase inhibition (Fig. 5). Similarly, treatment with the Sec61 inhibitor PS3061 increased cell-surface levels of BCMA in primary patient cells approximately two-fold, while not affecting cell-surface levels of CD38 (Fig. 5).

Increased efficacy of BCMA-ADC when combined with Sec61 inhibitor

Immunotherapy agents such as antibody drug conjugates (ADC) are sensitive to changes in expression of target antigen (25). We developed an ADC targeting BCMA, HDP101 (26-28) that has proven efficacy in MM cell lines at sub-nanomolar concentrations. Here, we knocked down BCMA using two independent sgRNAs in CRISPRi expressing KMS11 cells (Supplementary Fig S4) and performed a dose-response assay using increasing concentrations of BCMA-ADC. Our results indicate that cell lines in which BCMA is knocked down no longer respond to the ADC, thus establishing that the therapy is dependent on expression levels of BCMA on the cell surface (Fig 6A). Moreover, when cells were pre-treated for 24 hrs with either the gamma secretase inhibitor RO4929097 or the Sec61 inhibitor PS3061 at concentrations increasing cell surface levels of BCMA (Fig. 6B), we observed increased efficacy of the BCMA-ADC on the myeloma cell lines (Fig 6C). These findings demonstrate that our CRISPR screen was able to identify druggable targets that enhance the efficacy of immunotherapy agents.

BCMA CAR-T cell co-culture screen reveals myeloma cell-intrinsic proteins that affect CAR-T efficacy

The successful development of CAR-T cell therapies for B cell malignancies and myeloma has revolutionized therapy for patients not responding to or relapsed from standard treatments. However, patients can also develop resistance to CAR-T cell therapies. Mechanisms underlying resistance include poor persistence of CAR-T cells, loss of antigen expression on cancer cells, or additional, antigen-independent mechanisms yet to be determined (10,29,30). A systematic understanding of these mechanisms will enable us to design potential combination therapies pre-empting resistance to CAR-T cell therapy. Here, we used our CRISPR screening platform to identify genes or pathways that control sensitivity and resistance of multiple myeloma cells to BCMA-targeted CAR-T cells.

First, we generated BCMA CAR-T cells by transducing CD8+ T cells with a lentiviral vector encoding a second generation CAR incorporating an anti-BCMA single chair variable fragment, CD8a signal peptide, 4-1BB costimulatory domain and CD3-zeta signaling domain (see Methods). We validated the activation of BCMA CAR-T cells in the presence of AMO1 cells (Fig. 7A), and their cytotoxicity against AMO1 cells (Fig. 7B). Knockdown of BCMA in AMO1 cells using two independent sgRNAs (Supplementary Fig. S5) reduced both activation and cytotoxicity of BCMA-targeted CAR-T cells (Fig. 7A-B). This finding indicated that the efficacy of the CAR-T cells depends on the cell-surface levels of BCMA in myeloma cells (Fig. 7A-B).

While the expression level of the target antigen is a major determinant of response to CAR-T cells, there are likely also antigen-independent determinants. To systematically identify such determinants, we conducted a CRISPRi screen to identify genes or pathways in myeloma cells determining response to BCMA CAR-T cells (Fig. 7C). AMO1 cells expressing the CRISPRi machinery and an sgRNA library targeting 12,838 genes (including kinases, phosphatases, cancer drug targets, apoptosis genes, mitochondrial genes and transcription factors) were grown as mono-culture or co-cultured with BCMA CAR-T cells at a ratio of 1:1. 24 hours later, the surviving cells were harvested and processed for next-generation sequencing.

This CRISPRi screen identified a substantial number of genes regulating sensitivity to CAR-T cells (Fig. 7E and Supplementary Table S5). Comparing BCMA cell-surface levels to CAR-T sensitivity for different sgRNAs targeting BCMA, we observed that surface levels correlated with sensitivity to BCMA CAR-T cells (Fig. 7D). For example, knockdown of subunits of the gamma secretase complex and genes involved in sialic acid biosynthesis pathways *GALE* and *GNE*, which change BCMA cell surface expression, also concordantly affected sensitivity to BCMA CAR-T cells (Fig. 7E-F).

Furthermore, the screen identified a different category of genes, knockdown of which affected sensitivity of AMO1 cells to BCMA CAR-T cells without affecting cell-surface levels of BCMA. These genes included intercellular adhesion molecule 1 (*ICAM1*), which functions in T cell activation(31), and DNA fragmentation factor subunit alpha (*DFFA*), which is required for caspase activation to trigger apoptosis (32). Knockdown of *ICAM1* or *DFFA* resulted in decreased CAR-T cell sensitivity. Conversely, knockdown of genes belonging to the family of diacyl glycerol kinases caused increased sensitivity to BCMA CAR-T cells (Fig. 7F). Intriguingly, diacyl glycerol kinases had previously been described as factors in CAR-T cells that increase CAR-T cell killing activity (33) but our study suggest that inhibition of diacyl glycerol kinases in cancer cells also enhances their sensitivity to CAR-T cells.

This screen thus identified potential pathways that can regulate sensitivity to CAR-T cells either through changing cell surface expression of the antigen, or through an antigen-independent mechanism.

Discussion

CRISPR-based genetic screens are powerful tools to define vulnerabilities of cancer cells and to uncover the determinants of their response to therapies. Previously, CRISPR screens have been used to identify novel immunotherapy target antigens (34), better understand immune checkpoint regulation (1), understand resistance mechanisms to different immunotherapies (2,35) and regulators of immune function (36).

Here, we demonstrate the potential of using CRISPR screens in two additional ways to improve our systematic understanding of the determinants of immunotherapy: FACS-based screening, based on the cell-surface expression of the targeted antigen, and survival-based screening of cancer cells in the presence of CAR-T cells directed against clinically relevant targets.

We used our CRISPRi/CRISPRa screening platform to systematically identify mechanisms for upregulation of BCMA, an immunotherapy target antigen in multiple myeloma and tested their potential as combinatorial treatments to increase efficacy to immunotherapy agents. Our study showed that in addition to gamma-secretase inhibition, pharmacological inhibition of Class II HDAC and the Sec61 complex upregulated BCMA in myeloma cell lines and patient samples. Importantly, we show that Sec61 inhibitor-induced BCMA upregulation can be exploited to enhance the efficacy of BCMA-targeted ADC against myeloma cells. Our data thus confirms the importance of cell-surface antigen levels in determining response to immunotherapy agents.

Our findings raise several mechanistic questions, which will be subject of future studies. In particular, it is not clear how SEC61 inhibition results in increased cell-surface levels of BCMA. SEC61 knockdown was previously shown to upregulate a subset of proteins (37). This effect on BCMA could be due to direct effects on the interaction of BCMA with the SEC61 complex, or due to indirect effects mediated by changes in other SEC61 clients.

Both SEC61 and HDAC7 are potential combination targets for BCMA-targeted immunotherapy. Our SEC61 inhibitor sensitized myeloma cells to BCMA-targeted ADC, paving the way for testing its potential as a combinatorial treatment with BCMA-targeted immunotherapy in preclinical mouse models. Knockdown of *HDAC7* and treatment of cells with Class II HDAC inhibitor resulted in upregulation of BCMA. However, general HDAC inhibitors such as panobinostat and the HDAC6-specific inhibitor, ricolinostat did not upregulate BCMA. These results highlight the importance of inhibiting specific HDACs, and provides a potential therapeutic use case for an HDAC7-specific inhibitor to enhance BCMA-targeted immunotherapy.

Our study establishes that CRISPR-based screens enable a systematic and scalable approach to identifying mechanisms of antigen expression. Uncovering pathways that regulate BCMA transcription, translation and trafficking to the cell surface enables us to propose effective treatment strategies in patients with low basal expression of BCMA or following relapse due to antigen-loss. Clinical trials are currently ongoing to investigate the combination of gamma-secretase inhibitor with BCMA CAR-T cell therapy (NCT03502577). However, it is likely that not all patients would respond similarly to gamma secretase inhibition, or resistance may also develop to this combination strategy. Therefore, identifying alternative ways to modulate BCMA, as we discover here, retains high clinical relevance. Our results also support the concept that strategies to upregulate antigen expression on cancer cells can enhance efficacy of antigen-targeted immunotherapy agents.

Using a complementary strategy, our CRISPRi-CAR-T coculture screen uncovered both antigen-dependent and independent mechanisms in multiple myeloma cells that control the response to BCMA-targeted CAR-T cells. In particular, our screen showed that knockdown of diacylglycerol kinase (*DGK*) family of genes resulted in increased sensitivity to CAR-T cells. Previous groups have shown that inhibition of DGK-α activity in T cells using pharmacological inhibitors induced T cell activation, thus improving its cytotoxic activity on cancer cells (33,38). Our study indicates that knockdown of *DGK* kinases in myeloma cells increases sensitivity to T cells. This indicates that inhibitors against this family of kinases may be beneficial in CAR-T cell therapy of multiple myeloma through a dual mechanism, acting by both increasing T cell activity but also sensitizing myeloma cells to CAR-T cells.

Our study also identified genes in the sialic acid biosynthesis pathways, *GALE* and *GNE*, knockdown of which sensitized multiple myeloma cells to CAR-T cells. Although our BCMA-expression screen identified these genes to upregulate BCMA, the effect size of sensitizing the cells to CAR-T cells was much higher than the change in BCMA expression, indicating that there could be additional mechanisms by which this pathway modulates response to CAR-T cells. Sialic acid blockade in cancer cells has been shown to create an immune-permissive tumor microenvironment increasing CD8+ T cell activity (39). Therefore, inhibition of GALE and/or GNE could modulate the tumor microenvironment and increase sensitivity to CAR-T cells in an antigen-independent mechanism.

In summary, we present two complementary screening approaches to identify potential combinatorial treatments that can enhance the efficacy of immunotherapy through antigen-dependent and -independent mechanisms. These strategies should be readily adaptable to a broad range of cancer cell types, antigens, and immunotherapy modalities.

Materials and Methods:

Cell culture and CRISPR cell line generation

Multiple myeloma cell lines AMO1 (gift from Christoph Driessen, Kantonsspital St. Gallen, Switzerland) , KMS11 (JCRB), KMS12-PE (JCRB), OPM2 (DSMZ) and RPMI8226-luciferase (gift from Diego Acosta-Alvear, UCSB) (40) were grown in RPMI1640 complete growth media containing 10% fetal bovine serum (# 97068-085, Lot# 076B16, Seradigm), 1% Penicillin/Streptomycin (#15140122, Life tech) and 2 mM L-Glutamine (#25030081, Life tech). Cell lines were seeded at 0.2-0.4*10^6 cells/ml and passaged when they reached 1*10^6 cells/ml cell density. All cell lines were validated by STR profiling service provided by Genetica DNA Laboratories. To establish cell lines expressing functional CRISPRi, the multiple myeloma cell lines were lentivirally transduced with pMH0006 (41) and polyclonal cell lines were established by fluorescence-activated cell sorting (FACS) for BFP-positive cells. CRISPRi activity was validated using sgRNA targeted towards a cell surface marker, *CD38* (Supplementary Table S6). Briefly, CRISPRi MM cells expressing CD38 sgRNA or non-targeting control sgRNA were stained on day 10 post transduction using PE/Cy7 conjugated CD38 (HIT2) antibody (#303515, Biolegend) and analyzed for changes in levels of CD38 by flow cytometry using BD FACSCelesta™ (BD Biosciences).

For establishing CRISPRa cell line, AMO1 cells were lentivirally transduced with pMJ467-pHR-dCas9-HA-XTEN-VPR-2XP2A-mCherry (gift from James Nunez, Marco Jost and Jonathan Weissman, sequence available at kampmannlab.ucsf.edu/resources). This plasmid is an optimized version of JKNp44 (42), in which a universal chromatin opening

element was included upstream of the SFFV promoter, the linker between dCas9 and the VPR domain was replaced by an XTEN linker, and BFP was replaced by mCherry. Transduced cells were flow sorted based on mCherry fluorescence to generate a polyclonal cell line. CRISPRa activity was determined as described for CRISPRi using sgRNA targeted towards cell surface marker, *CXCR4* (Supplementary Table S6).

CRISPRi and CRISPRa flow cytometry screen

The genome-wide CRISPRi and CRISPRa v2.0 libraries subdivided into seven sublibraries containing five sgRNAs per gene were described previously(15). For pooled screening, sgRNA libraries were packaged into lentivirus for transduction into multiple myeloma cell lines as follows. Seven 15-cm dishes were seeded with $9*10^6$ HEK293T cells in 25 ml DMEM complete growth media. The next day each plate was transfected with 5 μg of sgRNA sublibrary (15) and 5 μg of third generation packaging mix (43) using Mirus TransIT-Lenti reagent (#MIR6600, Mirus Bio). Two days later, the viral supernatant was harvested and filtered through a 0.45 μm filter. Cold lentivirus precipitating solution (#VC100, Alstem, Inc.) was added at a final 1X concentration, mixed well and stored at 4°C overnight. Following incubation, the virus solution was centrifuged at 1500 g for 30 minutes at 4°C and the viral pellet was resuspended in cold RPMI media to transduce myeloma cells.

For transduction of each sublibrary, $30*10^6$ AMO1 cells expressing the CRISPRi or CRISPRa machinery were resuspended in 18 ml of virus containing medium with 8 μg/ml of polybrene. The cells were distributed into 6-well dishes and spin-infected at 700 g for 2 hrs at 32°C and allowed to recover for 3 hrs in the incubator. The cells were then harvested, washed twice with PBS and seeded at a concentration of $0.5*10^6$ cells/ml. 48 hrs later the cells were analyzed for percentage of infection by flow cytometry and treated with 1 μg/ml of puromycin to obtain a pure population of sgRNA expressing cells. On day 12 and day 5 post infection with the CRISPRi and CRISPRa sublibraries, cells were stained for cell surface BCMA and flow sorted to enrich for populations of cells expressing low or high cell surface levels of BCMA. Briefly, for each sublibrary, $80\text{-}100*10^6$ cells were harvested and washed once with PBS and resuspended in FACS buffer (PBS containing 0.5% FBS) at a concentration of $10*10^6$ cells/ml. The cells were blocked using Human BD Fc Block (#564220; BD Biosciences) for 15 mins to minimize background staining; stained with PE/CY7 conjugated BCMA (19F2) (#357508, Biolegend) antibody for an hour and resuspended in FACS buffer for flow sorting. Top and bottom 30% of cells expressing BCMA as determined from PE/Cy7 BCMA histogram were flow sorted using BD FACS Aria II. The different cell populations were then processed for next-generation sequencing as described previously (14,43) and sequenced on an Illumina HiSeq-4000. To identify significant hit genes, sequencing reads were analyzed using the MAGeCK-iNC pipeline as described previously(44).

CRISPRi validation screen

sgRNAs targeting the selected 41 top hits identified from the primary CRISPRi screen were cloned into a custom library of 90 sgRNAs, including two sgRNAs per gene and 8 non-targeting control sgRNAs. The sgRNAs were packaged into lentivirus as described for the primary screen and transduced into a panel of multiple myeloma cell lines (KMS11, AMO1, RPMI8226, OPM2 and KMS12-PE) expressing the CRISPRi machinery. The validation screen was carried out similar to the primary screen. Briefly, sgRNA expressing cells were individually stained using PE/Cy7 conjugated BCMA or FITC conjugated CD38 (#303504, Biolegend) and flow sorted to

enrich for antigen-high and antigen-low populations using BD FACS Aria II flow sorter. The frequencies of cells expressing a given sgRNA was determined by next-generation sequencing as described previously (14,43,44). Knockdown phenotypes for both BCMA and CD38 were hierarchically clustered based on Pearson correlation using Cluster 3.0 (45) and Java TreeView 3.0 (http://jtreeview.sourceforge.net/)(46).

Drug treatment of cells and staining for flow cytometry

For drug treatment, multiple myeloma cells were seeded at a concentration of $0.2*10^6$ cells/ml and treated with indicated concentration of TMP269 (#S7324; Selleckchem), Panobinostat (#S1030; Selleckchem), Ricolinostat (#S8001; Selleckchem), RO4929097 (#S1575; Selleckchem) for 48 hrs and with the Sec61 inhibitors, CT8 (22) and PS3061(24) for 24 hrs. Following drug treatment, cells were harvested and analyzed by flow cytometry for cell surface expression of BCMA and CD38. Briefly, $0.1*10^6$ cells were resuspended in 100 µl of FACS buffer and blocked using Fc block to minimize background staining. The cells were then stained with PE/Cy7 conjugated BCMA (19F2), FITC conjugated CD38 (HIT2) and propidium iodide (#P3566, Invitrogen) or corresponding isotype control antibodies (#400253; #400107, Biolegend) and analyzed by flow cytometry using BD FACS Celesta™ (BD Biosciences). Flow cytometry data was analyzed using FlowJo v10.4 (FlowJo), raw median fluorescence intensity (MFI) values of BCMA and CD38 stained cells were normalized to isotype control stained samples and data plotted as fold change in MFI relative to untreated cells using Prism V7 (GraphPad Software).

Western blotting

Total cell lysates were collected by resuspending cells in RIPA buffer (#89900, Thermo Fisher Scientific) supplemented with 1X protease inhibitor cocktail (#11836170001, Roche). Protein concentration was determined using BCA assay (#23225, Thermo Fisher Scientific) and protein extracts were prepared in SDS sample buffer at a concentration of 5 mg/ml. Equal concentrations of the cell lysates were loaded onto a NuPage 4-12% Bis-tris gels (#NP0336BOX, Thermo Fisher Scientific) and transferred onto a 0.45 µm pore nitrocellulose membrane using the Trans-Blot Turbo Transfer System (#1704270, Bio-Rad Laboratories, Inc.). The primary antibodies used in this study include: rabbit anti-BCMA (E6D7B) (#88183, Cell Signaling Technology), 1:2000; mouse anti-GAPDH (0411) (#sc-47724, Santa Cruz Biotechnology), 1:5000. Blots were incubated with Li-Cor secondary antibodies and imaged using Odyssey Fc imaging system (#2800, Li-Cor). Digital images were processed and analyzed using Li-Cor Image Studio software.

Quantitative-PCR (qPCR)

Drug treated cells or CRISPRi cells expressing sgRNA were harvested by centrifugation, and RNA extracted using the Quick-RNA miniprep kit (#R1054, Zymo Research). 1 µg of total RNA was reverse transcribed using Superscript III First-Strand Synthesis system (#18080051, Invitrogen). qPCR was performed using SensiFast SYBR Lo-ROX 2X qPCR master mix (#BIO-94005, Bioline) following manufacturers guidelines. Each qPCR reaction was set up in triplicates and run on Quantstudio 6 Flex (Applied Biosystems) following manufacturers protocol. Expression fold changes were calculated using the delta-delta Ct method and normalized to an internal control (beta-actin). The qPCR primers used are listed in Supplementary Table S6.

Multiple myeloma patient culture and drug treatments

De-identified primary MM bone marrow aspirates were obtained from the UCSF hematological malignancy tissue bank in compliance with the UCSF IRB protocols. Bone marrow mononuclear cells (BM-MNCs) were isolated by density gradient centrifugation using Histopaque-1077 (#10771, Sigma-Aldrich). Briefly, 3 ml of bone marrow aspirate was diluted with D-PBS without Calcium and Magnesium to a final volume of 8 ml and carefully laid over 3 ml of Histopaque-1077 and centrifuged at 400 g for 30 mins at room temperature. The layer containing plasma cells was carefully isolated, washed with PBS and resuspended in RPMI complete growth media to a concentration of $0.5\text{-}1*10^6$ cells/ml. For drug treatment, $0.1\text{-}0.2*10^6$ cells were seeded per well in a 96 well low binding plate (#650-185, Greiner). Cells were treated in triplicates for 24 hrs with indicated concentrations of drugs or DMSO. Following drug treatments, cells were stained using PE/Cy7 BCMA (19F2), FITC CD38 (HIT2), APC-R700 CD138 (MI15) (#566050, BD Biosciences) antibodies and propidium iodide or their corresponding isotype control antibodies and analyzed by flow cytometry using Bio-Rad ZE5 cell analyzer.

Antibody drug conjugate dose response assays

Myeloma cells were seeded at a concentration of $0.2*10^6$ cells/ml in a 96 well plate. For drug combination studies, cells were treated with either DMSO or indicated concentration of drugs prior to seeding. Increasing concentrations of the BCMA-targeted ADC HDP-101 were then added to cells to obtain a dose response curve. HDP-101 was produced as described previously (27,28). 96 hrs post treatment, cell viability was measured using CellTiter-Glo 2.0 reagent (#G9241, Promega) following manufacturer's protocol. Raw luminescence signals were collected using a SpectraMax M5 plate reader (Molecular Devices). All measurements were taken in triplicates and raw counts were normalized as the percent of signal relative to untreated cells or percent maximum signal when comparing more than one drug. Sigmoidal dose-response curve fitting for IC_{50} calculation was performed using Prism V7 package (GraphPad software Inc.).

ELISA assay

To determine soluble BCMA (sBCMA) levels in the cell culture supernatant, solid phase sandwich ELISA using polyclonal goat antibodies was used (#DY193, Human BCMA/TNFRSF17 Duoset ELISA, R&D Systems). Cell culture supernatant was harvested from cells treated with indicated concentration of drugs by centrifugation and serially diluted in the recommended reagent diluent and concentration of sBCMA was determined following the manufacturer's instructions.

Generation of CAR construct

To generate the BCMA-targeted CAR, the nucleotide sequence for the BCMA-50 scFv (Patent: https://patents.google.com/patent/US20170183418) and a N-terminal CD8a signal peptide plus myc-tag was synthesized. Using Gibson cloning, the CAR was assembled by fusing the BCMA-50 scFv to the CD8a hinge and transmembrane domain, 4-1BB costimulatory domain, the CD3-zeta chain, and a C-terminal EGFP. The CAR was then inserted into the second generation lentiviral vector pHR-SIN. The CD19 CAR has been previously described (47).

Isolation of CD8+ T cells

De-identified donor blood after apheresis was obtained from Blood Centers of the Pacific (San

Francisco, CA) as approved by UCSF IRB policies. CD8+ T cells were isolated from donor blood using EasySep ™ Human CD8+ T cell isolation kit (#19053, Stemcell Technologies) following the manufacturers protocol. Purified CD8+ T cells were cryopreserved in RPMI1640 media supplemented with 20% human AB serum (#HP1022, Valley Medical) and 10% DMSO (#D2650, Sigma) solution. For experiments, T cells were cultured in Ex-Vivo 15 media (#04-418Q, Lonza) supplemented with 5% human AB serum, 10mM neutralized N-acetyl L-Cysteine (#A9165, Sigma Aldrich), 1X beta-mercaptoethanol (#21985-023, Thermo Fisher Scientific) and 50 units/ml of recombinant human IL-2 (#200-02, Peprotech).

Generation of CAR-T cells and cytotoxicity assay

For CAR-T cell generation, lentivirus was produced in HEK293T cells by transfecting pHR'SIN:CAR-Transgene vector and lentiviral packaging plasmids, pMD2.G and pCMVdR8.9 using Mirus TransIT-Lenti transfection reagent. Viral supernatant was harvested 48 hr after transfection and precipitated using Alstem lentivirus precipitating solution. Primary CD8+ T cells were thawed and 24 hrs later the cells were stimulated with Dynabeads Human T-Expander CD3/CD28 beads (#11141D, ThermoFisher Scientific) at a cell:bead ratio of 1:2. The following day, primary T cells are exposed to the precipitated virus for 24 hrs. On day 5 post stimulation, Dynabeads were removed and GFP CAR-T cells were enriched by FACS sorting using BD FACS Aria II. The sorted CAR-T cells were maintained in culture until day 10-12 when they are used for downstream assays.

For T cell cytotoxicity assays, GFP-CAR-T cells were co-cultured in the presence of BFP-CRISPRi multiple myeloma cells at an Effector:Target (E:T) ratio of 1:1 for 24 hrs. Baseline target cell death was measured by incubating CRISPRi myeloma cells without any effector cells over the same time period. After incubation, cells were washed and stained with BV786-CD69 (FN50) (#310932, Biolegend) to determine T cell activation status and propidium iodide to assess overall cell death. Flow cytometry analysis was performed on GFP-positive CAR-T cells to determine changes in CD69 cell surface levels and myeloma cell cytotoxicity was determined by calculating the percentage change in BFP-positive multiple myeloma cells in the presence or absence of effector cells.

CRISPRi-CAR survival screen

AMO1 CRISPRi cells expressing an sgRNA library targeting 12,838 genes (including kinases, phosphatases, cancer drug targets, apoptosis genes, proteastasis genes and mitochondrial genes) were co-cultured in the presence or absence of GFP-BCMA CAR-T cells at an E:T ratio of 1:1 for 24 hrs. Surviving cells were then harvested and the different cell populations were processed for next generation sequencing as described previously (14,43). Sequencing reads were analyzed using MAGeCK-iNC pipeline developed in our lab to identify significant hit genes as described (44).

Author contributions

Conception and design: P Ramkumar, AP Wiita, M Kampmann
Development of methodology: P Ramkumar, M Seyler, J Leong, M Chen, KT Roybal
Acquisition of data: P Ramkumar, M Seyler, J Leong, M Chen, N Shah, SW Wong, T Martin, JL Wolf, KT Roybal, J Taunton
Analysis and interpretation of data: P Ramkumar, R Tian, J Taunton, AP Wiita, M Kampmann

Writing, review and/or revision of the manuscript: P Ramkumar, M Kampmann
Administrative, technical, or material support: J Leong, P Choudhry, T Hechler, N Shah, SW Wong, T Martin, JL Wolf, KT Roybal, A Pahl, J Taunton
Study supervision: P Ramkumar, M Kampmann
Other (Contribution of unpublished materials): T Hechler, KT Roybal, A Pahl, J Taunton

Acknowledgements
We thank James Nunez, Marco Jost, Christina Liem and Jonathan Weissman for sharing their unpublished CRISPRa construct; Diego Acosta-Alvear for sharing mCherry-Luciferase RPMI8226 cell line; Axel Hyrenius-Wittsten and Joe Hiatt for inputs on T cell culturing; Eric Chow and Derek Bogdanoff (UCSF Center for Advanced Technology) for support with next-generation sequencing; Sarah Elmes and Jane Gordon (UCSF Laboratory for Cell Analysis) for support with FACS; Stratton Georgoulis, Molly Bassette and Logan Hille for contributing to preliminary studies. For primary patient samples, we thank Nina Shah, Sandy W. Wong, Tom G. Martin III, Jeffrey L. Wolf and the Grand Multiple Myeloma Translational Initiative. We thank all the co-authors and members of the Kampmann lab for discussion and feedback on the manuscript.

References Cited

1. Burr ML, Sparbier CE, Chan YC, Williamson JC, Woods K, Beavis PA, *et al.* CMTM6 maintains the expression of PD-L1 and regulates anti-tumour immunity. Nature **2017**;549:101-5
2. Tsui CK, Barfield RM, Fischer CR, Morgens DW, Li A, Smith BAH, *et al.* CRISPR-Cas9 screens identify regulators of antibody-drug conjugate toxicity. Nat Chem Biol **2019**;15:949-58
3. Majzner RG, Mackall CL. Tumor Antigen Escape from CAR T-cell Therapy. Cancer Discov **2018**;8:1219-26
4. Iorgulescu JB, Braun D, Oliveira G, Keskin DB, Wu CJ. Acquired mechanisms of immune escape in cancer following immunotherapy. Genome Med **2018**;10:87
5. Nijhof IS, Casneuf T, van Velzen J, van Kessel B, Axel AE, Syed K, *et al.* CD38 expression and complement inhibitors affect response and resistance to daratumumab therapy in myeloma. Blood **2016**;128:959-70
6. Pont MJ, Hill T, Cole GO, Abbott JJ, Kelliher J, Salter AI, *et al.* gamma-secretase inhibition increases efficacy of BCMA-specific chimeric antigen receptor T cells in multiple myeloma. Blood **2019**
7. Bu DX, Singh R, Choi EE, Ruella M, Nunez-Cruz S, Mansfield KG, *et al.* Pre-clinical validation of B cell maturation antigen (BCMA) as a target for T cell immunotherapy of multiple myeloma. Oncotarget **2018**;9:25764-80
8. Cho SF, Anderson KC, Tai YT. Targeting B Cell Maturation Antigen (BCMA) in Multiple Myeloma: Potential Uses of BCMA-Based Immunotherapy. Front Immunol **2018**;9:1821

9. Laurent SA, Hoffmann FS, Kuhn PH, Cheng Q, Chu Y, Schmidt-Supprian M*, et al.* gamma-Secretase directly sheds the survival receptor BCMA from plasma cells. Nat Commun **2015**;6:7333
10. Raje N, Berdeja J, Lin Y, Siegel D, Jagannath S, Madduri D*, et al.* Anti-BCMA CAR T-Cell Therapy bb2121 in Relapsed or Refractory Multiple Myeloma. N Engl J Med **2019**;380:1726-37
11. Susanibar Adaniya SP, Cohen AD, Garfall AL. Chimeric antigen receptor T cell immunotherapy for multiple myeloma: A review of current data and potential clinical applications. Am J Hematol **2019**;94:S28-S33
12. Brudno JN, Maric I, Hartman SD, Rose JJ, Wang M, Lam N*, et al.* T Cells Genetically Modified to Express an Anti-B-Cell Maturation Antigen Chimeric Antigen Receptor Cause Remissions of Poor-Prognosis Relapsed Multiple Myeloma. J Clin Oncol **2018**;36:2267-80
13. Cohen AD, Garfall AL, Stadtmauer EA, Melenhorst JJ, Lacey SF, Lancaster E*, et al.* B cell maturation antigen-specific CAR T cells are clinically active in multiple myeloma. J Clin Invest **2019**;129:2210-21
14. Gilbert LA, Horlbeck MA, Adamson B, Villalta JE, Chen Y, Whitehead EH*, et al.* Genome-Scale CRISPR-Mediated Control of Gene Repression and Activation. Cell **2014**;159:647-61
15. Horlbeck MA, Gilbert LA, Villalta JE, Adamson B, Pak RA, Chen Y*, et al.* Compact and highly active next-generation libraries for CRISPR-mediated gene repression and activation. Elife **2016**;5
16. Zhao C, Inoue J, Imoto I, Otsuki T, Iida S, Ueda R*, et al.* POU2AF1, an amplification target at 11q23, promotes growth of multiple myeloma cells by directly regulating expression of a B-cell maturation factor, TNFRSF17. Oncogene **2008**;27:63-75
17. Luistro L, He W, Smith M, Packman K, Vilenchik M, Carvajal D*, et al.* Preclinical profile of a potent gamma-secretase inhibitor targeting notch signaling with in vivo efficacy and pharmacodynamic properties. Cancer Res **2009**;69:7672-80
18. Ding ZM, Liu YG. [Effects of phosphoramidothiolate pesticides on rat erythrocyte membrane acetylcholinesterase]. Zhonghua Yu Fang Yi Xue Za Zhi **1988**;22:82-4
19. Lobera M, Madauss KP, Pohlhaus DT, Wright QG, Trocha M, Schmidt DR*, et al.* Selective class IIa histone deacetylase inhibition via a nonchelating zinc-binding group. Nat Chem Biol **2013**;9:319-25
20. Scuto A, Kirschbaum M, Kowolik C, Kretzner L, Juhasz A, Atadja P*, et al.* The novel histone deacetylase inhibitor, LBH589, induces expression of DNA damage response genes and apoptosis in Ph- acute lymphoblastic leukemia cells. Blood **2008**;111:5093-100
21. Santo L, Hideshima T, Kung AL, Tseng JC, Tamang D, Yang M*, et al.* Preclinical activity, pharmacodynamic, and pharmacokinetic properties of a selective HDAC6 inhibitor, ACY-1215, in combination with bortezomib in multiple myeloma. Blood **2012**;119:2579-89
22. Mackinnon AL, Paavilainen VO, Sharma A, Hegde RS, Taunton J. An allosteric Sec61 inhibitor traps nascent transmembrane helices at the lateral gate. Elife **2014**;3:e01483
23. Garrison JL, Kunkel EJ, Hegde RS, Taunton J. A substrate-specific inhibitor of protein translocation into the endoplasmic reticulum. Nature **2005**;436:285-9

24. Shah PS, Link N, Jang GM, Sharp PP, Zhu T, Swaney DL*, et al.* Comparative Flavivirus-Host Protein Interaction Mapping Reveals Mechanisms of Dengue and Zika Virus Pathogenesis. Cell **2018**;175:1931-45 e18
25. Collins DM, Bossenmaier B, Kollmorgen G, Niederfellner G. Acquired Resistance to Antibody-Drug Conjugates. Cancers (Basel) **2019**;11
26. Pahl A, Lutz C, Hechler T. Amanitins and their development as a payload for antibody-drug conjugates. Drug Discov Today Technol **2018**;30:85-9
27. Pahl A, Ko J, Breunig C, Figueroa V, Lehners N, Baumann A*, et al.* HDP-101: Preclinical evaluation of a novel anti-BCMA antibody drug conjugates in multiple myeloma. Journal of Clinical Oncology **2018**;36:e14527-e
28. Figueroa-Vazquez V. KJ, Breunig C., Baumann, A.,Giesen N., Pálfi A., Müller C., Lutz C., Hechler T., Kulke M., Mueller-Tidow C., Goldschmidt H., Pahl A., Raab MS. HDP-101, a novel anti-BCMA antibody-drug conjugate, specifically kills proliferating and resting multiple myeloma cells. Submitted
29. Shah NN, Fry TJ. Mechanisms of resistance to CAR T cell therapy. Nat Rev Clin Oncol **2019**;16:372-85
30. Xu J, Chen LJ, Yang SS, Sun Y, Wu W, Liu YF*, et al.* Exploratory trial of a biepitopic CAR T-targeting B cell maturation antigen in relapsed/refractory multiple myeloma. Proc Natl Acad Sci U S A **2019**;116:9543-51
31. Wingren AG, Parra E, Varga M, Kalland T, Sjogren HO, Hedlund G*, et al.* T cell activation pathways: B7, LFA-3, and ICAM-1 shape unique T cell profiles. Crit Rev Immunol **1995**;15:235-53
32. Gu J, Dong RP, Zhang C, McLaughlin DF, Wu MX, Schlossman SF. Functional interaction of DFF35 and DFF45 with caspase-activated DNA fragmentation nuclease DFF40. J Biol Chem **1999**;274:20759-62
33. Riese MJ, Moon EK, Johnson BD, Albelda SM. Diacylglycerol Kinases (DGKs): Novel Targets for Improving T Cell Activity in Cancer. Front Cell Dev Biol **2016**;4:108
34. Dong MB, Wang G, Chow RD, Ye L, Zhu L, Dai X*, et al.* Systematic Immunotherapy Target Discovery Using Genome-Scale In Vivo CRISPR Screens in CD8 T Cells. Cell **2019**;178:1189-204 e23
35. Han P, Dai Q, Fan L, Lin H, Zhang X, Li F*, et al.* Genome-Wide CRISPR Screening Identifies JAK1 Deficiency as a Mechanism of T-Cell Resistance. Front Immunol **2019**;10:251
36. Shifrut E, Carnevale J, Tobin V, Roth TL, Woo JM, Bui CT*, et al.* Genome-wide CRISPR Screens in Primary Human T Cells Reveal Key Regulators of Immune Function. Cell **2018**;175:1958-71 e15
37. Nguyen D, Stutz R, Schorr S, Lang S, Pfeffer S, Freeze HH*, et al.* Proteomics reveals signal peptide features determining the client specificity in human TRAP-dependent ER protein import. Nat Commun **2018**;9:3765
38. Noessner E. DGK-alpha: A Checkpoint in Cancer-Mediated Immuno-Inhibition and Target for Immunotherapy. Front Cell Dev Biol **2017**;5:16
39. Bull C, Boltje TJ, Balneger N, Weischer SM, Wassink M, van Gemst JJ*, et al.* Sialic Acid Blockade Suppresses Tumor Growth by Enhancing T-cell-Mediated Tumor Immunity. Cancer Res **2018**;78:3574-88

40. Lam C, Ferguson ID, Mariano MC, Lin YT, Murnane M, Liu H*, et al.* Repurposing tofacitinib as an anti-myeloma therapeutic to reverse growth-promoting effects of the bone marrow microenvironment. Haematologica **2018**;103:1218-28
41. Chen JJ, Nathaniel DL, Raghavan P, Nelson M, Tian R, Tse E*, et al.* Compromised function of the ESCRT pathway promotes endolysosomal escape of tau seeds and propagation of tau aggregation. J Biol Chem **2019**
42. Tak YE, Kleinstiver BP, Nunez JK, Hsu JY, Horng JE, Gong J*, et al.* Inducible and multiplex gene regulation using CRISPR-Cpf1-based transcription factors. Nat Methods **2017**;14:1163-6
43. Kampmann M, Bassik MC, Weissman JS. Functional genomics platform for pooled screening and generation of mammalian genetic interaction maps. Nat Protoc **2014**;9:1825-47
44. Tian R, Gachechiladze MA, Ludwig CH, Laurie MT, Hong JY, Nathaniel D*, et al.* CRISPR Interference-Based Platform for Multimodal Genetic Screens in Human iPSC-Derived Neurons. Neuron **2019**
45. Eisen MB, Spellman PT, Brown PO, Botstein D. Cluster analysis and display of genome-wide expression patterns. Proc Natl Acad Sci U S A **1998**;95:14863-8
46. Saldanha AJ. Java Treeview--extensible visualization of microarray data. Bioinformatics **2004**;20:3246-8
47. Imai C, Mihara K, Andreansky M, Nicholson IC, Pui CH, Geiger TL*, et al.* Chimeric receptors with 4-1BB signaling capacity provoke potent cytotoxicity against acute lymphoblastic leukemia. Leukemia **2004**;18:676-84

Figures and Figure legends

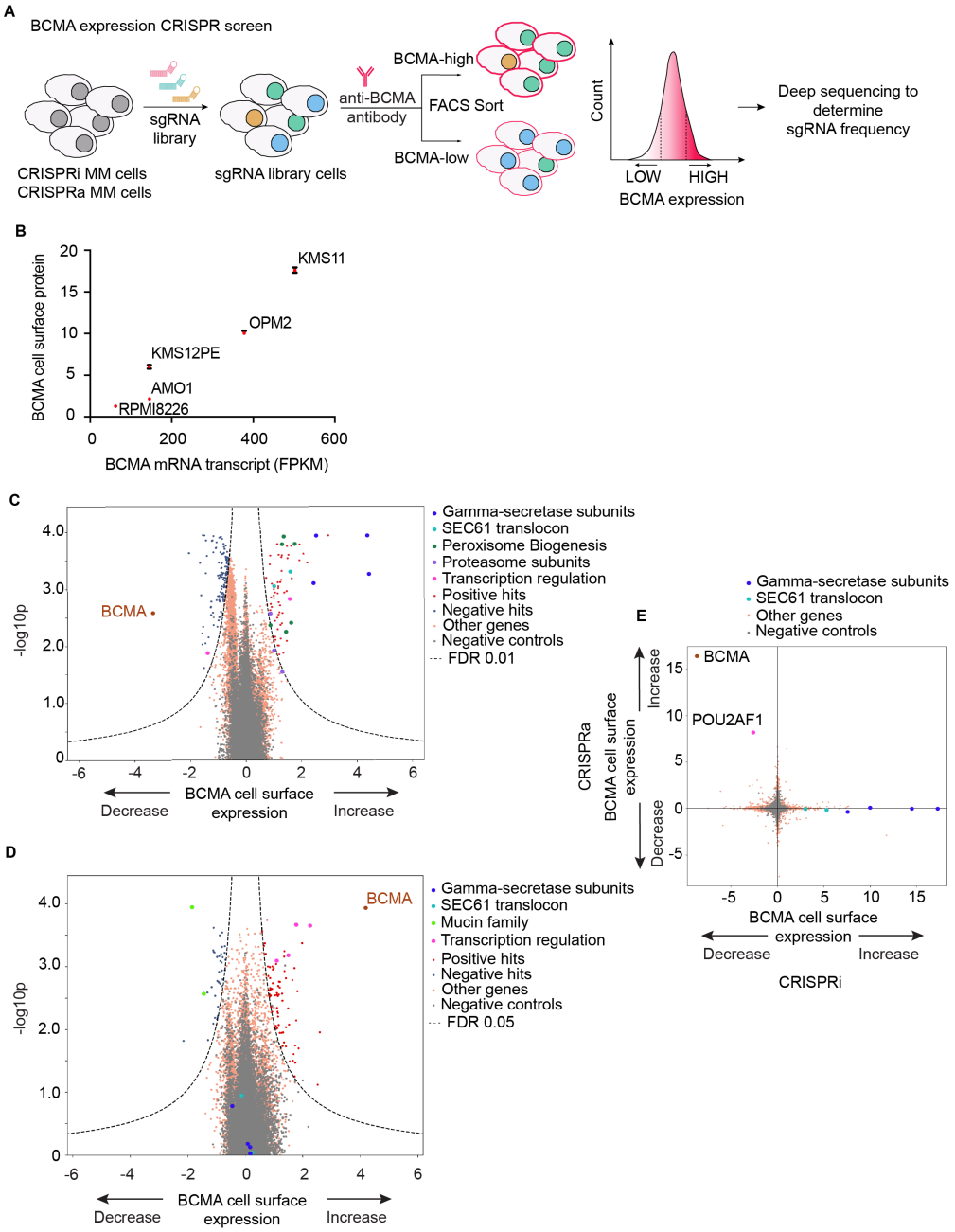

Fig 1:

Genome-wide CRISPRi/a screens to identify genes regulating cell-surface expression of BCMA

A, Schematic representation of our genome-wide CRISPRi and CRISPRa screens to identify modulators of BCMA expression. AMO1 cells constitutively expressing the CRISPRi or CRISPRa machinery were transduced with genome-wide lentiviral sgRNA library. Following transduction, cells were stained for cell surface levels of BCMA and sorted by fluorescence-activated cell sorting (FACS) to enrich for populations with low or high levels of cell surface BCMA. Frequencies of cells expressing a given sgRNA were determined in each population by

next generation sequencing. **B,** BCMA expression levels in a panel of MM cell lines. BCMA transcript FPKM levels obtained from the Keats lab database: https://www.keatslab.org were plotted against cell surface expression levels of BCMA quantified by flow cytometry. The flow cytometry data are means of three biological replicates, error bars denote SD. Note that some error bars are not visible because values are small. **C and D,** Volcano plots indicating the BCMA expression phenotype and statistical significance for knockdown (CRISPRi, C) or overexpression (CRISPRa, D) of human genes (orange dots) and quasi-genes generated from negative control sgRNA (grey dots). Hits genes corresponding to functional categories are color-coded as labeled in the panel. **E,** Comparison of phenotypes from the CRISPRi and CRISPRa screens. Selected hit genes are color-coded.

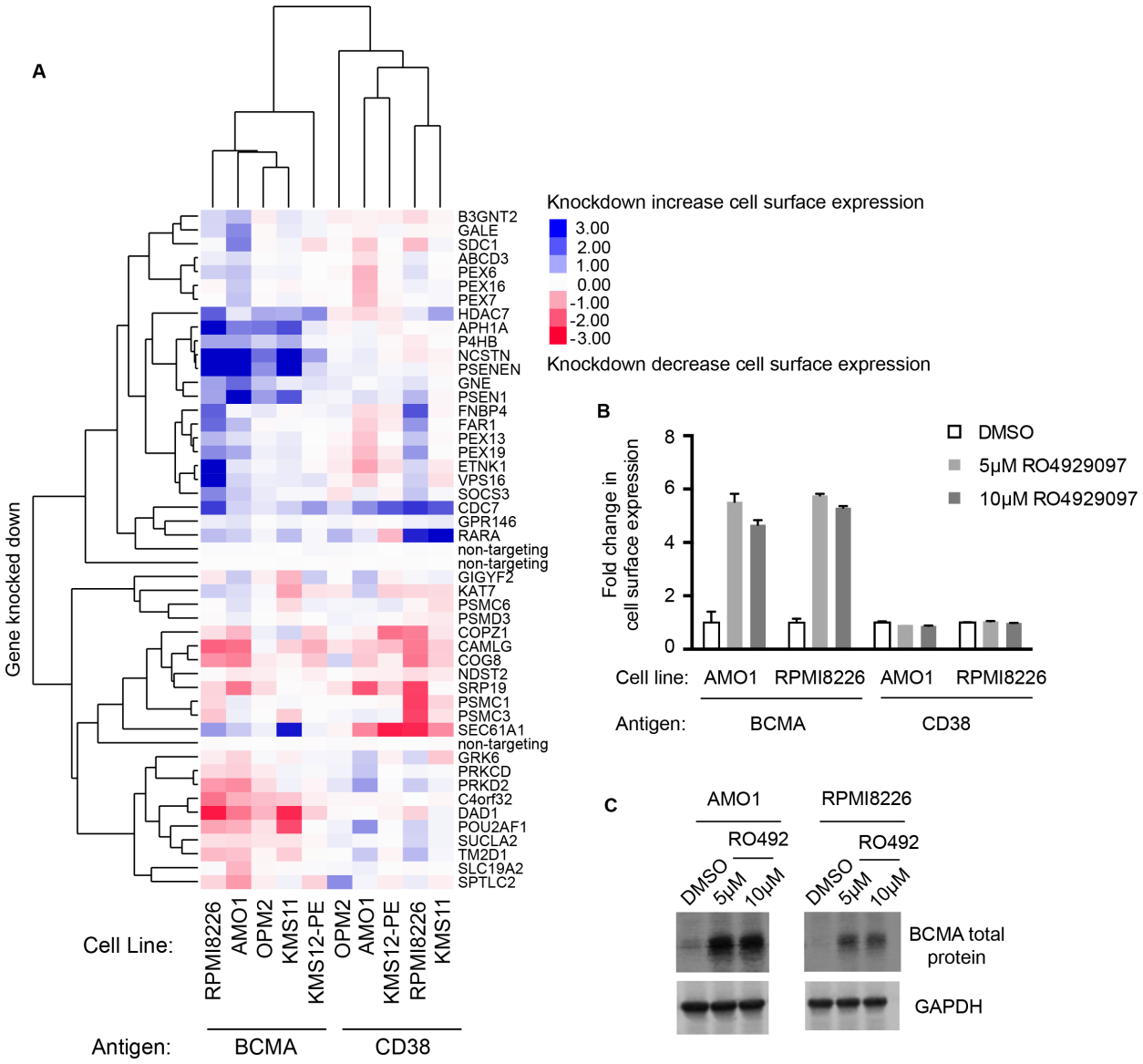

Fig 2:

Validation of hit genes from the primary screen. **A,** Heat map representation of knockdown phenotype scores from CRISPRi validation screens in a panel of MM cell lines, for cell-surface levels of BCMA and CD38. Both genes and screens were hierarchically clustered based on Pearson correlation. **B and C,** AMO1 and RPMI8226 cells treated with indicated concentrations of the gamma-secretase inhibitor RO4929097 or DMSO for 48 hrs were analyzed by flow cytometry (B) and immunoblotting (C) for changes in BCMA levels. (B) Fold changes in BCMA cell surface levels were determined by normalizing to DMSO-treated cells. Data points are means of three biological replicates; error bars denote SD. (C) Western blot of endogenous BCMA. GAPDH was used as a loading control.

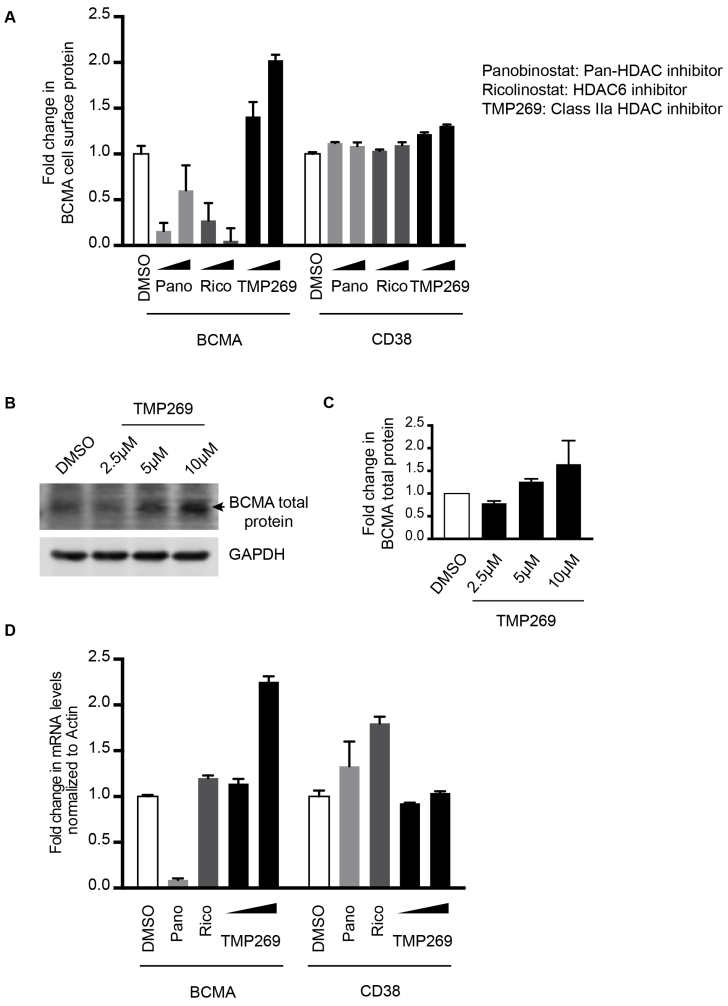

Fig 3:

Class IIa-HDAC inhibition increases transcription of BCMA **A,** RPMI8226 cells were treated with increasing concentrations of the pan HDAC inhibitor panobinostat (10 nM, 25 nM); the HDAC6-specific inhibitor ricolinostat (0.5 μM, 1 μM); the class II-HDAC inhibitor TMP269 (5 μM, 10 μM), or DMSO for 48 hrs and analyzed by flow cytometry for cell surface expression of BCMA and CD38. Fold changes in protein levels were determined by normalizing to the DMSO-treated cells. Data points are means of three biological replicates; error bars denote SD. **B and C,** Total protein extracts from RPMI8226 cells treated with 2.5 μM, 5 μM and 10 μM of TMP269 for 48 hrs were analyzed by immunoblotting for expression levels of BCMA. GAPDH was used to normalize differences in loading amounts. Data is represented as fold change relative to the total protein expression level after normalization with GAPDH. Data points are means of two technical replicates, error bars denote SD. **D,** RPMI8226 cells treated with 10 nM panobinostat, 0.5 μM ricolinostat and 5 μM and 10 μM of TMP269 for 48 hrs were processed for quantitative PCR (qPCR) to determine transcript levels of BCMA and CD38. Fold changes in transcript levels with different drug treatments were determined after normalizing to beta-actin gene. Data are means of two biological replicates, error bars denote SD.

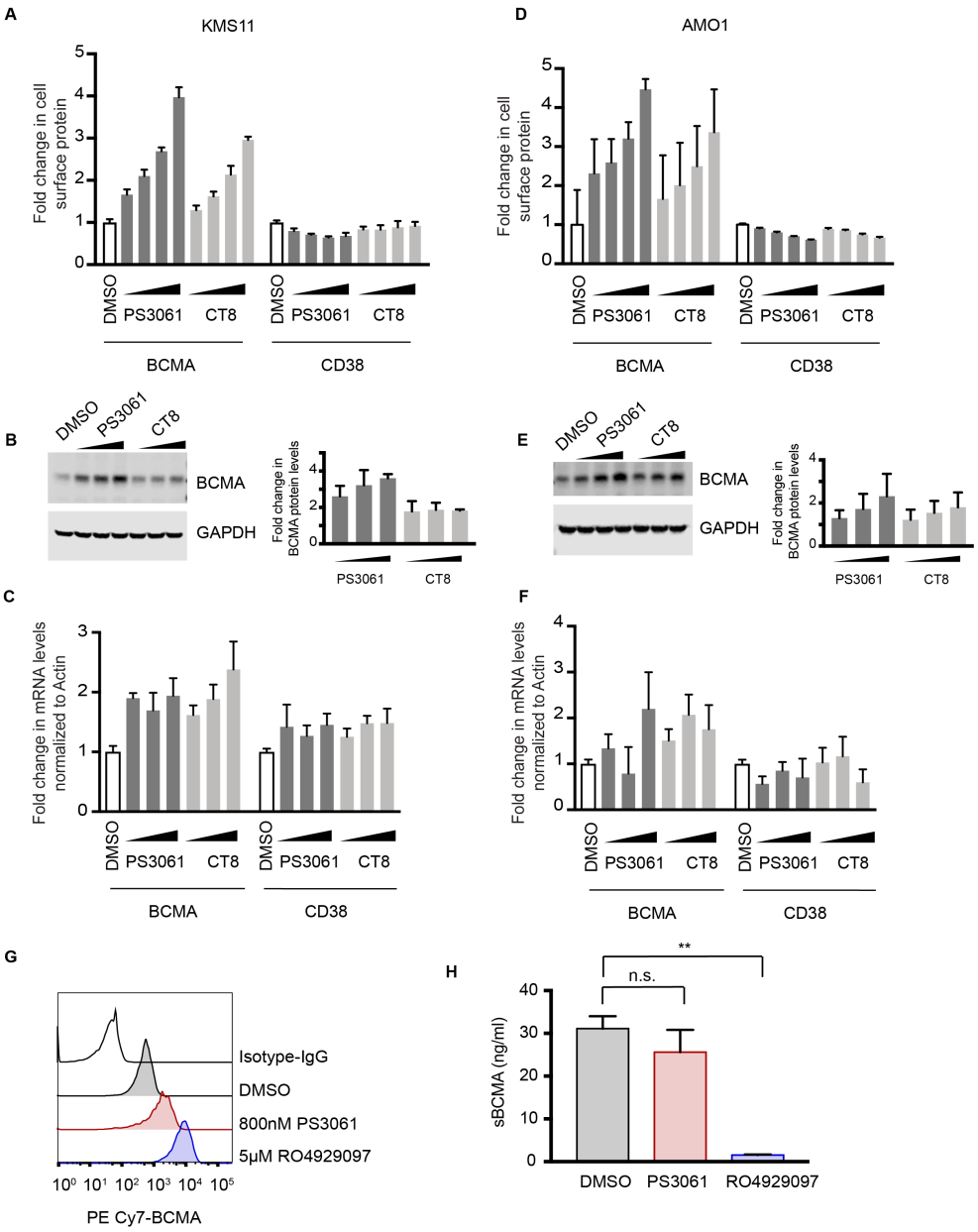

Fig 4:

Sec61 inhibitors increase cell-surface expression of BCMA in KMS11 (A-C) and AMO1 (D-F) cells **A and D,** KMS11 and AMO1 cells were treated with increasing concentrations of Sec61 inhibitors, CT8 and PS3061 (100, 200, 400, 800 nM) or DMSO as a control for 24 hrs. Cells were stained for cell surface expression of BCMA and CD38 and analyzed by flow cytometry. Data are means of three biological replicates; error bars denote SD. **B and E,** Total protein lysates from cells treated with increasing concentration of CT8 and PS3061 (200, 400, 800 nM) for 24 hrs were processed for western blotting. GAPDH was used to normalize for differences in loading amounts. Data is represented as fold change relative to the normal protein expression level after normalization with GAPDH. Data points are means of two technical replicates, error bars denote SD. **C and F,** cells treated with increasing concentrations of PS3061 and CT8 (200, 400, 800 nM) for 24 hrs were processed for qPCR to determine transcript levels of BCMA and

CD38. Fold change in transcript levels were determined after normalizing to beta-actin. Data are means of two biological replicates, error bars denote SD. **G and H,** KMS11 cells were treated with 800 nM PS3061, 5 μM RO4929097 and DMSO for 24 hrs. G, Drug-treated cells were analyzed by flow cytometry for cell surface expression of BCMA. Histograms indicate distribution of PE/CY7 BCMA in the drug-treated cells. Data is a representation of two biological replicates. H, Soluble BCMA (sBCMA) concentration in the cell culture supernatant post drug treatment was measured using ELISA. Data are means of two biological replicates, error bars denote SD. *$P < 0.005$, n.s. - not significant, two-tailed unpaired t test.

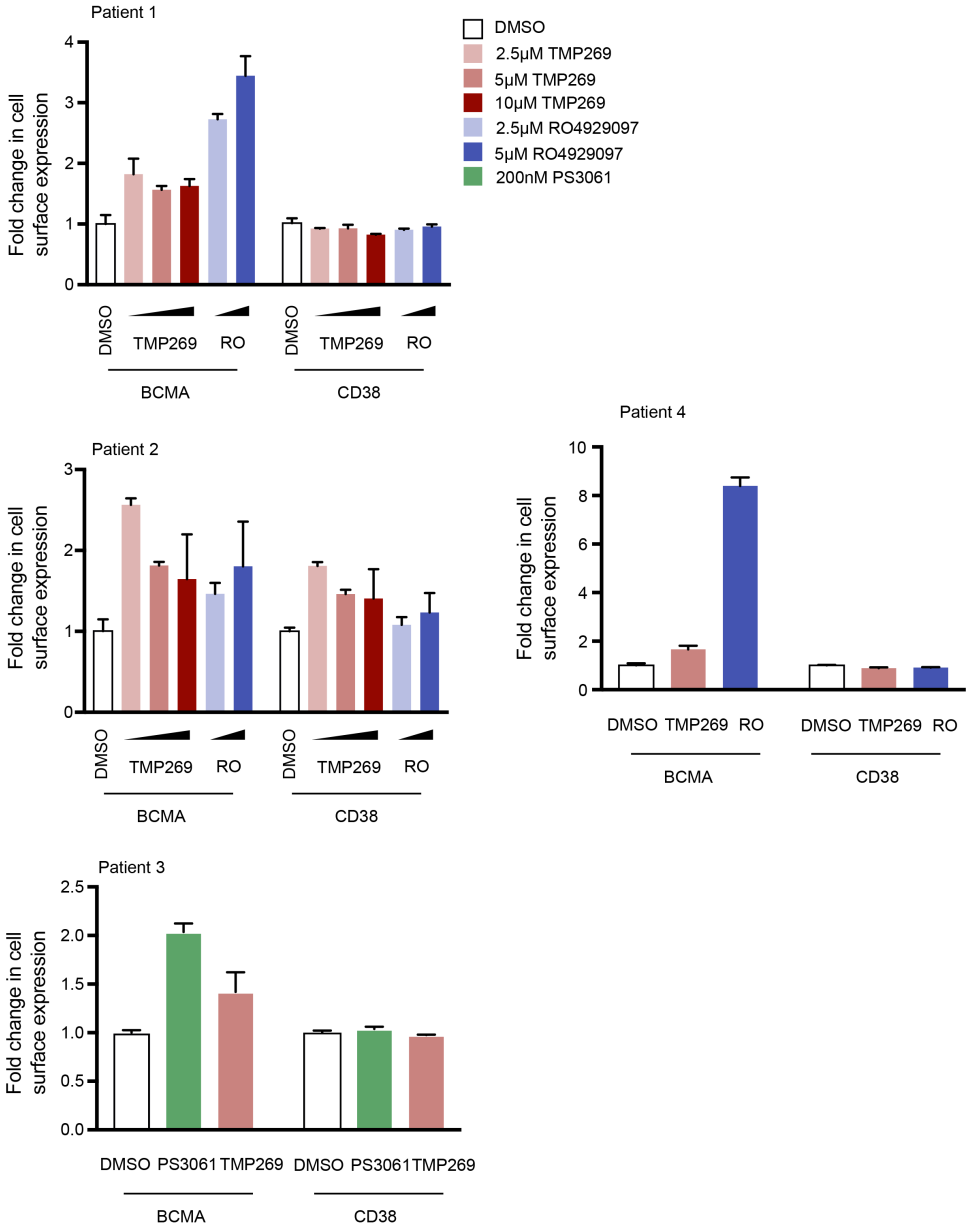

Fig 5:

Pharmacological inhibition of the validated hits in myeloma patient samples upregulate cell-surface BCMA levels. Bone marrow-mononuclear cells (BM-MNCs) isolated from bone marrow aspirates from different MM patients were treated with indicated concentration of Class II-HDAC inhibitor, TMP269; gamma-secretase inhibitor, RO4929097; and Sec61 inhibitor, PS3061 for 24 hrs. Cells were stained for cell-surface CD138, BCMA and CD38 and analyzed by flow cytomtery. Fold change in BCMA and CD38 levels were determined in CD138+ live cell populations. Data are means of three technical replicates, error bars denote SD.

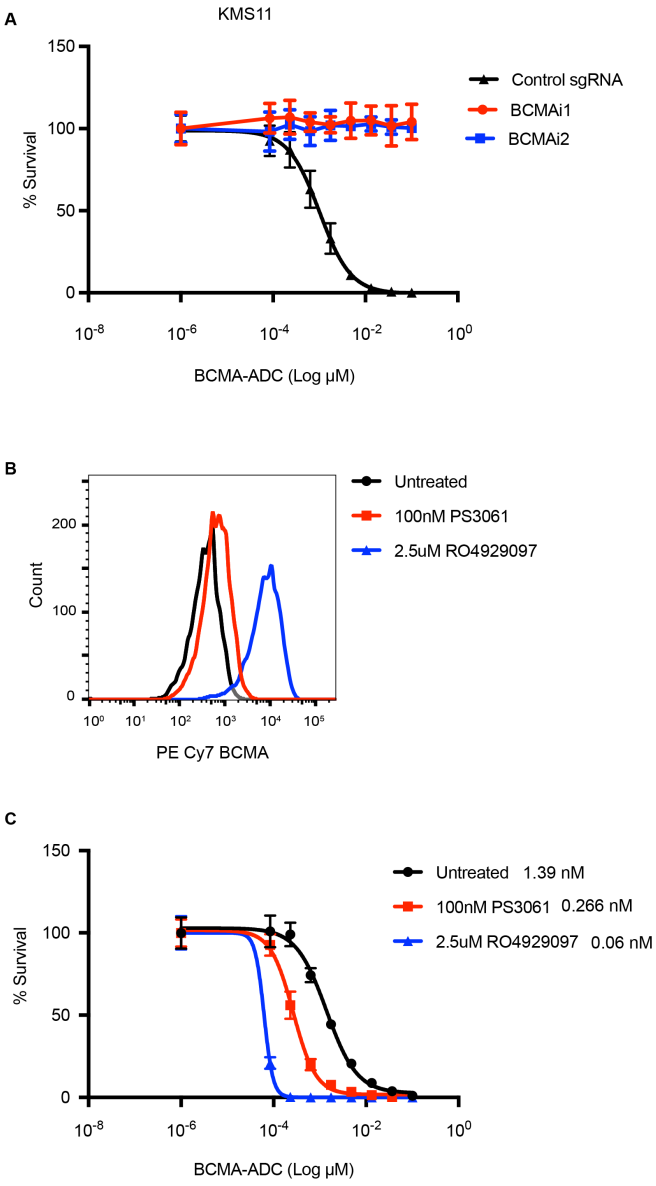

Fig 6:

Increased efficacy of BCMA-ADC when combined with Sec61 inhibitor **A**, BCMA-ADC cytotoxicity dose-response assay of CRISPRi KMS11 cells expressing two independent sgRNA targeted towards BCMA and a non-targeting control sgRNA. **B,** KMS11 cells treated with indicated concentrations of PS3061 and RO4929097 were stained for BCMA and analyzed by flow cytometry. Histograms indicate the distribution of BCMA. Data is a representation of two biological replicates. **C,** BCMA-ADC cytotoxicity dose-response assay was performed in combination with indicated concentrations of drugs. Data points are means of two biological replicates; error bars denote SD.

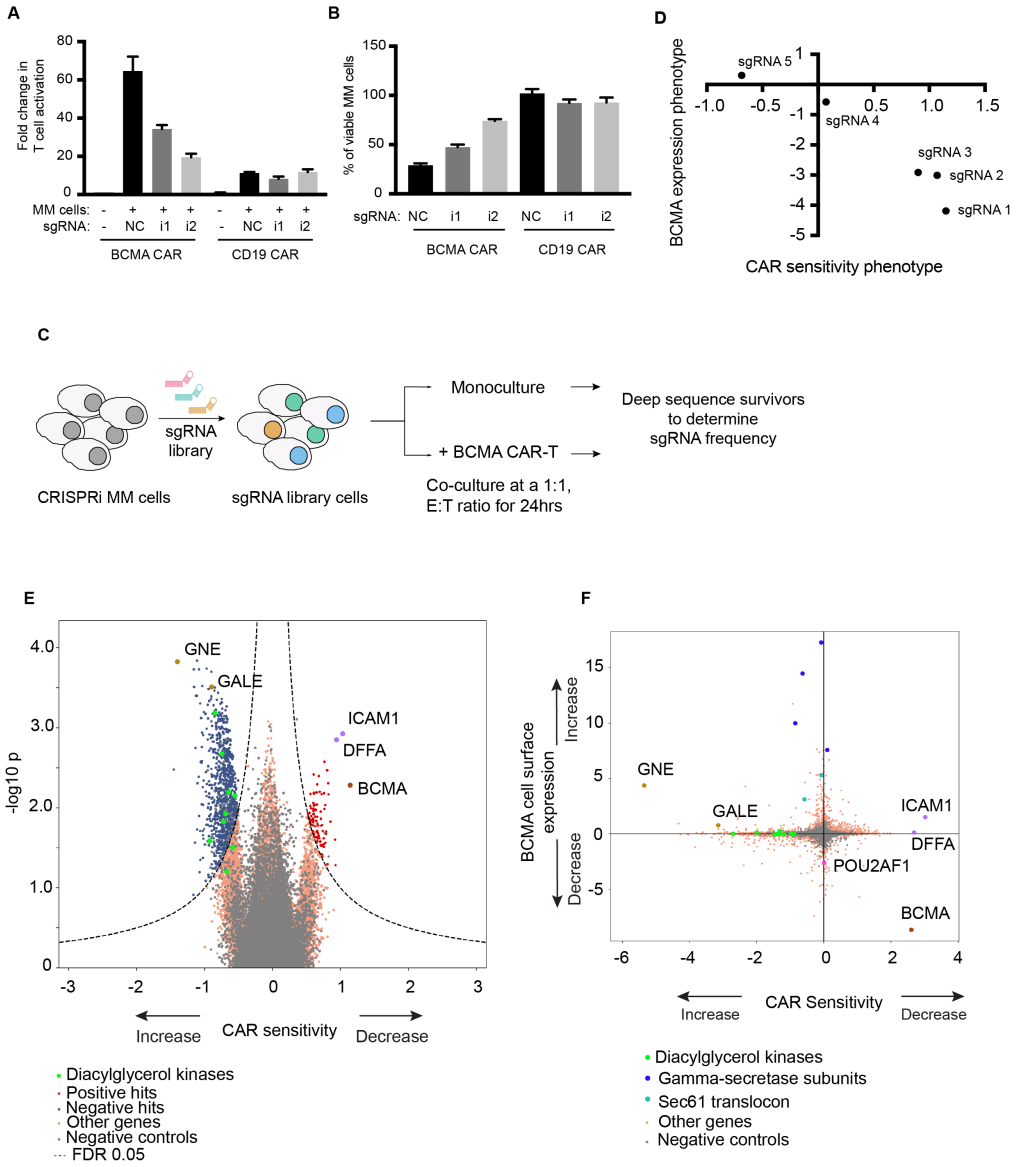

Fig 7:

CRISPRi-CAR-T screen identifies genes modulating response to BCMA CAR-T cells **A and B,** CRISPRi AMO1 cells expressing BFP-sgRNA targeted towards BCMA or non-targeting control sgRNA were co-cultured at a 1:1 ratio with BCMA- or CD19- GFP CAR-T cells. Fold changes in T cell activation was determined by analyzing for cell surface expression of CD69 on T cells normalized to CD69 expression on resting T cells. Myeloma cell viability was determined by propidium iodide staining of BFP-positive myeloma cells. **C,** Schematic representation of the CRISPRi-CAR-T cell co-culture screen. **D,** Comparison of BCMA expression phenotype to sensitivity towards BCMA-CAR indicating different sgRNAs targeted towards BCMA. **E,** Volcano plot indicating CAR-T sensitivity phenotypes and statistical significance of knockdown of human genes (orange dots) and quasi-genes from negative control sgRNAs (grey dots) in

multiple myeloma cells. Hits genes corresponding to functional categories are color-coded as labeled in the panel. **F,** Comparison of BCMA expression phenotype from the CRISPRi primary screen (Fig. 1) to sensitivity towards BCMA-CAR. Hits genes corresponding to functional categories are color-coded as labeled in the panel.